2012 IEEE/RSJ International Conference on
Intelligent Robots and Systems
October 7-12, 2012. Vilamoura, Algarve, Portugal

# Velvet Fingers: A Dexterous Gripper with Active Surfaces.

Vinicio Tincani[†], Manuel G. Catalano[†‡], Edoardo Farnioli[†‡], Manolo Garabini[†],
Giorgio Grioli[†], Gualtiero Fantoni[†] and Antonio Bicchi[†‡]

*Abstract*— **The design of grasping and manipulation systems is one of the most investigated topics in recent robotic and automation engineering. It is a process that has to take into account many development possibilities and to face different trade offs, as that between application possibilities and design complexity.**

**In this work we present the design of a novel end-effector that merges the essential mechanics and control simplicity of underactuated devices, together with the high levels of manipulability usually featured in dexterous robotic hands. To obtain this enhancement, the proposed gripper considers the possibility offered by active surfaces, i.e. engineered contact surfaces able to simulate different levels of friction and to apply tangential thrust to the contacted object. The actual dexterity enhancement is evaluated by an analytical manipulability analysis and some examples of in hand manipulations and grasps are taken into account. A mechanical solution is presented, which implements the proposed idea through the adoption of one DoF active surfaces mounted on the fingers. The proposed solution presents a manipulability index one order of magnitude higher than common grippers.**

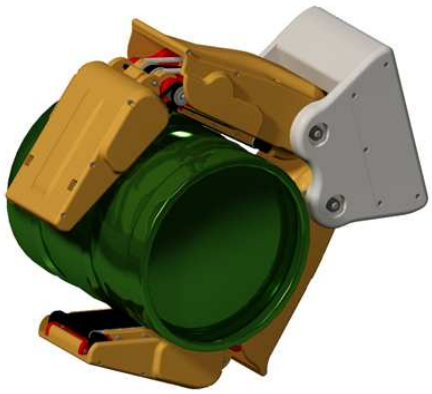

Fig. 1. 3D render of the "Velvet Fingers" smart gripper grasping a small beer keg.

## I. INTRODUCTION

Over the years, engineers proposed many different devices with the purpose of grasping and manipulating objects: from simple industrial grippers to fully actuated anthropomorphic robotic hands, which are collectively identified by the term End Effectors (EEs).

Simple grippers, characterized by one or two actuated Degrees of Freedoms (DoFs), find extensive application in industry. In most cases they are designed for grasping one well-defined object (see [1]), and cannot grasp objects of different shapes or dimensions, they also lack in-hand manipulation capabilities.

Salisbury's three-fingered robotic hand [2] and the Utah/MIT hand [3] are the first two prototypes of EE that showed manipulation capabilities. Since their introduction, many different designs have been proposed, from very simple devices [4], to multi-fingered hands such as the UB Hand IV [5], to very sophisticated fully actuated devices that incorporate the ultimate advancements in robotic actuation, such as [6]. Extensive surveys on robot hand systems exist, as for instance those reported in [7] and [8].

At least two points of view stand out in literature of robotic hand design: one approach (e.g. see [5] and [6]) attempts to replicate the human hand capabilities by imitating its mechanical structure. This comes at the cost of very complex mechanism design and control algorithms. The other approach specializes the designed hand to obtain some desired grasp shape and/or manipulation feature. For instance, a number of multi-fingered under-actuated devices (e.g. [10]) has been presented, according to the latter philosophy.

A recent framework, proposed as an aid to deal with control and design issues of robotic hands, is that of synergies (see [11] and [12]). Not only this approach establishes a foundation to manage the very large number of DoFs of an anthropomorphic robot hand, but it can also be exploited to under-actuate EEs while preserving suitable grasping and manipulation features. In particular the concept of soft synergies (see [12]) highlights the importance of incorporating in the EE adaptability to the object being grasped.

A possible direction for further improvement of end-effector design for grasping and manipulation, that we start exploring in this paper, is the introduction of *active surfaces*. The idea of using active surfaces at the finger-pads is prompted by the successful developments in adhesive surface engineering. Bio-inspired designs, such as Cutkosky's Stickybot ([13], [14]), first produced a robot with the ability to climb on flat vertical surfaces, and later led to the development of the gecko-tape [15], an innovative product with many potential and practical applications in nano-technology, military, health care and sport sectors. The potential for grippers using extremely high adhesion is clearly very high, although it has been explored so far only to a limited extent, mostly in the micro/nano domain (see e.g. [16]). However, in many applications where the end-effector is required to quickly grasp and release the object, and also performs at least some simple in-hand manipulation tasks, high adhesion surfaces may not be enough.

The idea of active surfaces thus aims at controlling adhesion between the fingers and the object in different manipulation phases. Controlling adhesion would imply to be able to regulate it from very high ("sticky fingers") to very

[†] Interdepart. Research Center "E. Piaggio", University of Pisa, Via Diotisalvi, 2, 56100 Pisa, Italy.

[‡] Department of Advanced Robotics, Istituto Italiano di Tecnologia, via Morego, 30, 16163 Genova.

low ("slippy fingers"), thus enabling nimble manipulation with "velvet fingers". It is also conceivable, through the use of a suitably shaped surface adhesion wave, to apply tangential forces on the manipulated object to relocate it on the finger-pad (see Sec. II).

Summing everything up, the design of an EE is a process that has to take into account many possibilities and the trade-off between performances, in terms of grasping, manipulation, and complexity. In this paper we describe a preliminary attempt at exploiting the idea of adding dexterity to simple, under-actuated grippers through the adoption of active surfaces. While analogous conventional grippers include three or four actuated rotational joints, the proposed device substitutes two rotational actuators with two active surfaces. A manipulability analysis is performed, based on the Rayleigh quotient (see [17] and [18]), to compare the proposed solution with the conventional counterpart. Finally, after choosing the main design parameters, the presented solution is finalized in a prototype (see Fig. 1) where the control of adhesion is obtained by a simple device, i.e. high-friction finger pads which can move with one degree of freedom so as to simulate the effect of variable adhesion in one direction. The paper is organized as follows: in Sec. II the active adhesion surface concept is explained and analyzed; in Sec. III a description of the kinematics and main design parameters are provided and a manipulability analysis is portrayed; in Sec. IV the mechanical design is reported; finally, Sec. V presents conclusions and sketches the future work.

## II. ACTIVE SURFACES

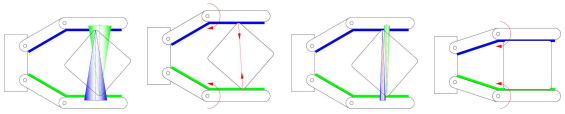


Fig. 2. Advantages of friction modulation: sticky behavior for increased tip grasping stability (a-b) and slippy behavior for in-hand grasp reconfiguration (c-d).

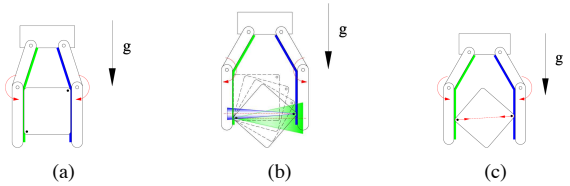


Fig. 3. In-hand grasp reconfiguration with modulated friction and external forces (in this example gravity).

Among the many possibilities offered by active surfaces, this work will take into account i) the ability to change friction and ii) the ability to tangentially push a surface in contact. These possibilites can increase the dexterity of under-actuated hands and dexterous grippers, combining the typical robustness of low DoFs grippers with the dexterity featured by a high DoFs hands. For instance, Fig. 2 shows how controllable friction can be used to decide the

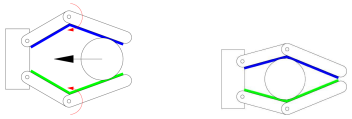


Fig. 4. Controlled slipping between active surfaces and grasped object for smooth tip-grasp to power-grasp transition.

evolution of a tip grasp configuration: keeping it stable with high friction (2(a), 2(b)), or letting the object slide toward a different grasp through controlled slipping (2(c) and 2(d)). Fig. 3 shows another example of in-hand grasp reconfiguration where the combined use of active surfaces and external forces (in this example gravity) allows to go back from the grasp configuration of Fig. 2(d) to the original configuration of 2(a). Fig. 4 shows an example of active surface operation during grasping: low friction allows the object translation from a configuration with two contact points to a configuration with four contact points. On the

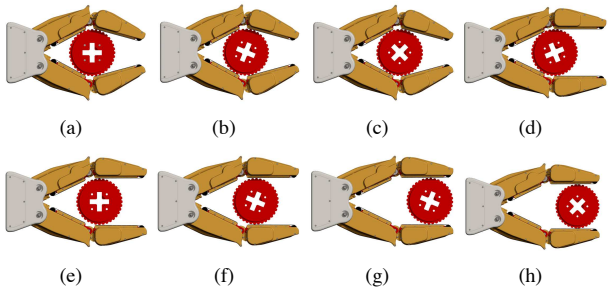


Fig. 5. Manipulation enhancement by using pushing active surfaces. Pictures show how the grasped object can be rotated (a, b, c, d), translated (f,g), or simultaneously rotated and translated (e,h), combining the two movements.

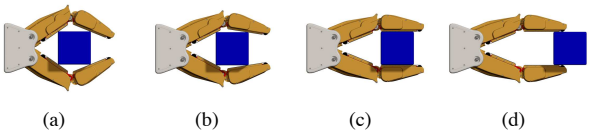


Fig. 6. Controlled object expulsion using pushing active surfaces. The grasped object (a) is moved (b-c) untill it is completely expelled out of the hand (d). Adaptability of the under-actuated gripper guarantees grasp stability during the whole movement.

other hand, the possibility to tangentially push the object through the active surface allows other kinds of in-hand manipulations, as rotations and translations, as shown in Fig.s 5 and 6. In particular, Fig. 5 shows as pushing on the object from the active surface, in same or opposite verses, it is possible to rotate (a,b,c,d), to translate (f,g), or to combine the two motions (e,h) on a grasped object. Fig. 6 shows a controlled expulsion of an object realized by the active surfaces of the fingers only. The grasped object (a) is moved by means of a coordinate action of the active surfaces (b) and is pushed towards the finger tips (c) till it is completely expelled out of the hand (d).

Different means can be imagined to implement the described possibilities of active surfaces. In Fig. 7 and 8

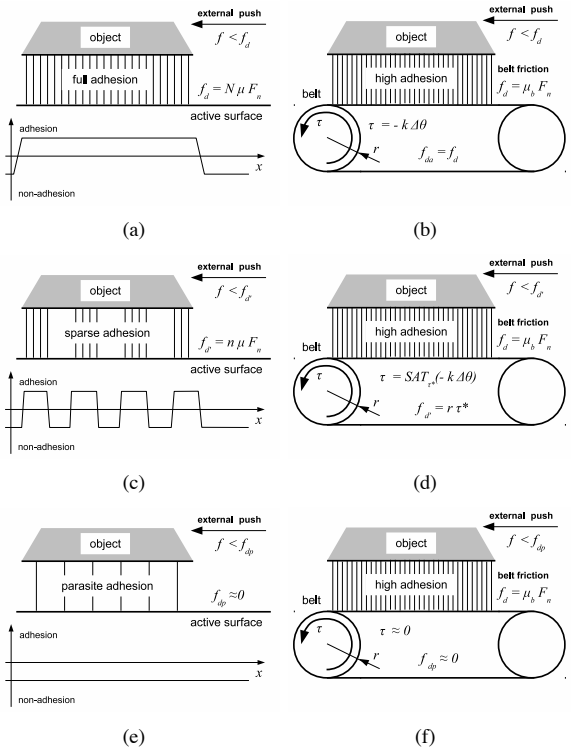


Fig. 7. Friction modulation with the two proposed active surfaces implementations: micro/nano adhesion element ensembles (left colum) and powered belt (right column). The three rows show three different levels of friction from high (top), through medium (middle), to low (bottom). A high static friction force $f_d$ can be achieved by activation of a large number $N$ of adhesion elements, or by a high gain $k$ negative feedback control on the motor of the conveyor. A medium level $f_{d'}$ of friction is obtained through selective activation of a smaller quantity $n$ of adhesion elements, or by saturation of the conveyor motor torque to a value $\tau^*$ (operation $SAT_{\tau^*}(\cdot)$ related to the desired friction by the conveyor pulley radius $r$. The minimum friction $f_{dp}$ that can be obtained is determined by the parasite friction of the non-active adhesion elements, or by the residual torque due to the conveyor motor gear friction and non-perfectly canceled dynamics.

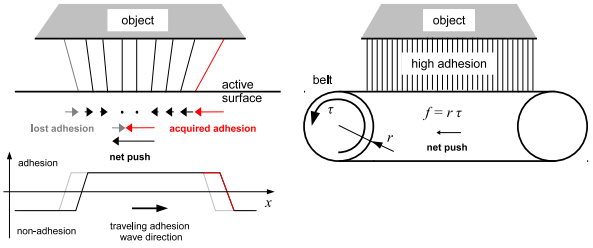


Fig. 8. Tangential push with the two proposed active surfaces implementations: coherent waves of adhesion elements (left colum) and belt activation (right column).

two possible implementations are shown, one relying on synchronized control of multiple active adhesion elements, the other, inspired by [19], based on actuation of a plane belt. Fig. 7 shows how different levels of friction can be implemented by the two solutions. In Fig.s 7(a), 7(c) and 7(e) progressive de-activation of the active adhesion surface is adopted to decrease the friction to very low levels. The same

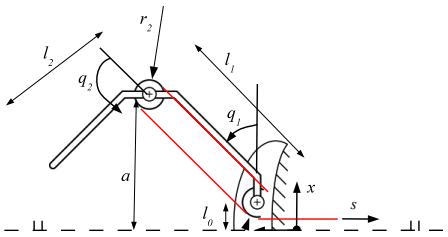

Fig. 9. Reference frames for the kinematic design and manipulability analysis of the proposed hand.

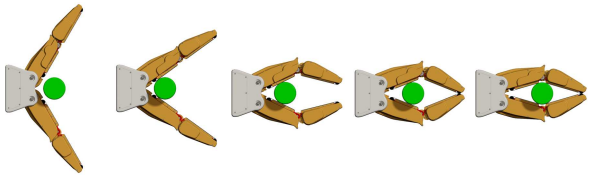


Fig. 10. Hand closing with an object in it (sequence). When the hand starts closing (a) the fingers keep moving straight until the first contact with the object (b). At this point, the distal phalanges start bending faster than the proximal (c) until the two fingertips touch each other (d). Proper transmission design ensures that, despite the tips interference, the hand keeps squeezing the object, reaching a grasp closure.

behavior can be obtained by changing the maximum torque allowed to a high gain controller to prevent the retrograde motion of the belt (Fig.s 7(b), 7(d), 7(f)). Fig. 8 shows that tangential pushes can be applied to contacted object, by simply applying a torque to the motor actuating the belt (Fig. 8(b)), or by applying traveling waves of adhesion which exploit local dynamics on the wave fronts to obtain a net push on the object. Given its simplicity for the 1 DoF case, the belt solution is adopted in the present work, nevertheless the authors believe that incoming developments in micro/nano scale adhesion control can, in the near future, tilt the scales of decision.

## III. VELVET FINGERS DESIGN

### A. Dexterous Gripper Design

The kinematic scheme of the proposed gripper is presented in Fig. 9. The two fingers are actuated by a single motor that moves the proximal and distal phalanxes by a transmission mechanism that drives their angles as in a differential mechanism. The kinematics of each finger-tip is described by

$$\begin{cases} x = l_0 + l_1\cos(q_1) + l_2\cos(q_1+q_2) \\ y = l_1\sin(q_1) + l_2\sin(q_1+q_2) \\ s = r_1 q_1 + r_2 q_2. \end{cases} \quad (1)$$

Symbols in (1) (which are defined in Fig. 9) represent the main design parameters of the EE. In particular $s$ is the generalized displacement of the motor actuating the finger. The parameters were chosen to grasp an object with the main dimension up to 200 mm. The length $l_0$ was chosen such that the gap between the fingers is about 1 mm in a parallel configuration, to allow the gripper to pick up also very small objects. Lengths $l_1$ and $l_2$ were determined by consequence, following the general guidelines described in [10]. Particular

attention was devoted to select the transmission ratios $r_1/r_2$. Indeed, because of the EE design, it could occur that after the two proximal phalanxes come in contact with the object and the two distal phalanxes touch each other (see Fig. 10(d)). If the motor keeps actuating the closure movement ($\delta s > 0$), two cases can happen: (i) fingers tend to straighten ($\delta q_1 > 0$), keeping the grasp, (ii) fingers tend to bend ($\delta q_1 < 0$), losing the grasp. We can say that case (ii) is avoided if the *closure condition* $\delta q_1/\delta s > 0$ holds for every $q_1, q_2$ belonging to the EE workspace.

By differentiating (1) we obtain

$$\begin{cases} \delta x = -l_1 \sin(q_1)\delta q_1 - l_2 \sin(q_1+q_2)(\delta q_1 + \delta q_2) \\ \delta y = l_1 \cos(q_1)\delta q_1 + l_2 \cos(q_1+q_2)(\delta q_1 + \delta q_2) \\ \delta s = r_1 \delta q_1 + r_2 \delta q_2. \end{cases} \tag{2}$$

Solving the third equation of (2) for $\delta q_2$, substituting it into the first, imposing $\delta x = 0$ for symmetry conditions, we obtain the relationship

$$\delta q_1 = \frac{l_2 \sin(q_1+q_2)/r_2}{l_2 \sin(q_1+q_2)\left(\dfrac{r_1}{r_2} - 1\right) - l_1 \sin(q_1)} \delta s. \tag{3}$$

Since, from design constraints, $0 < q_1 + q_2 < \pi$ and $\sin(q_1 + q_2) > 0$, the closure condition is satisfied when

$$\frac{r_1}{r_2} > \frac{l_1 \sin(q_1)}{l_2 \sin(q_1+q_2)} + 1\,. \tag{4}$$

To evaluate the second member of equation (4) we introduce the object dimension $a$ and have that

$$c \equiv \frac{l_1 \sin(q_1)}{l_2 \sin(q_1+q_2)} = \sqrt{\frac{l_1^2 - (a-l_0)^2}{l_2^2 - a^2}} \approx \sqrt{\frac{l_1^2 - a^2}{l_2^2 - a^2}}, \tag{5}$$

where $l_0$ was neglected since in our design it is $l_0 \ll l_1$ and $l_0 \ll l_2$. From relation (5) it appears that it is desirable to have $l_2 \geq l_1$ because in this case $c \leq 1$, hence, by (4), with a ratio $r_1/r_2 > 2$ the closure condition is satisfied.

### *B. Manipulability Analysis*

To better assess the dexterity increment derived by the adoption of active surfaces, a rigorous manipulability analysis is required, to perform which, the two finger active surfaces can be approximated by prismatic joints. Despite the fact that analytical instruments for manipulability analysis give results referring to local properties around an equilibrium configuration, studying more cases helps to better understand the global behavior of the system.

It is possible to demonstrate that a minimum set of equation describing the displacement of the system around an equilibrium configuration can be written in the form $A\delta y = 0$, thus as a *linear* and *homogeneous* set of equations[1]. The coefficient matrix $A \in \mathbb{R}^{r_a \times c_a}$ depends on the *Jacobian matrix*, the *grasp matrix* and the *synergy matrix*, describing the under-actuation of the system. The *augmented configuration variation* $\delta y \in \mathbb{R}^{c_a}$ is a vector incorporating: (i) the generalized system force vaiations, composed by those of the external wrench $\delta w$, the contact force variation $\delta f_c$, the generalized actuation torque $\delta \eta$, and (ii) the generalized configuration variations, composed by those of the object $\delta u$ and of the actuation variable $\delta \sigma$. Since $A$ is a fat matrix, we can introduce $\Gamma \in \mathbb{R}^{r_\gamma \times c_\gamma}$, with $r_\gamma = c_a$ and $c_\gamma = c_a - r_a$, as a basis for its nullspace, such that $\mathscr{R}(\Gamma) = \mathscr{N}(A)$. Although the matrix $\Gamma$ does not have a unique formulation, it can always be partitioned in two block columns, one relative to the *internal* perturbed configurations, when there is not any external wrench variation, and the other for the *external* perturbed configurations, when an external wrench variation occurs on the object. In other word we can say that all the solutions of the system are in the form

$$\begin{bmatrix} \delta w \\ \delta f_c \\ \delta \eta \\ \delta u \\ \delta \sigma \end{bmatrix} = \begin{bmatrix} 0 & \Gamma_{we} \\ \Gamma_{f_c i} & \Gamma_{f_c e} \\ \Gamma_{\eta i} & \Gamma_{\eta e} \\ \Gamma_{ui} & \Gamma_{ue} \\ \Gamma_{\sigma i} & \Gamma_{\sigma e} \end{bmatrix} \begin{bmatrix} x_i \\ x_e \end{bmatrix}. \tag{6}$$

This formulation is very useful in order to study the dexterity of a hand. In fact, as an index for the *internal kinematic manipulability*, it is possible to chose the ratio

$$R_{k_m i} = \frac{\delta u_i^{\mathrm{T}} \delta u_i}{\delta \sigma_i^{\mathrm{T}} \delta \sigma_i}, \tag{7}$$

where $\delta u_i$ and $\delta \sigma_i$ are displacements referred to an *internal* contact force variation. Taking into account the equation (6), and substituting the expression for the *internal object displacement* and the corresponding actuation variation in (7), it immediately follows that

$$R_{k_m i} = \frac{x_i^{\mathrm{T}} \Gamma_{ui}^{\mathrm{T}} \Gamma_{ui} x_i}{x_i^{\mathrm{T}} \Gamma_{\sigma i}^{\mathrm{T}} \Gamma_{\sigma i} x_i}. \tag{8}$$

The index (8) has the form of a *Rayleigh quotient* which has a maximum corresponding to the maximum eigenvalue $\lambda_{max}$ of the pencil $\Gamma_{ui}^{\mathrm{T}} \Gamma_{ui} - \lambda \Gamma_{\sigma i}^{\mathrm{T}} \Gamma_{\sigma i}$. The corresponding optimal direction in object displacement space is given by $\delta u_{max} = \Gamma_{ui} x_{i,max}$. Similar considerations are possible for the others eigenvalues and corresponding eigenvectors. To optimize the distribution of the degrees of actuation (DoAs) in the hand, the above instrument has been used to compare the manipulability of the kinematic structure. A tip grasp and a power grasp configuration were considered, both studied for the 3 DoAs and 4 DoAs cases. The resulting ellipsoids (ellipsis) are sketched in Fig. 11. Characteristic lengths of the ellipsoid axes are summarized in Table I.

The first column of the table lists the references to the right sub-figure. The second column identifies with a code the type of grasp, adopting the convention: *P* for a power grasp or *T* for a tip grasp, *A* if the hand has active surfaces or *Na* if it has not, and the number of actuation degrees. Since in these cases ellipsoid axis directions are very similar to the reference system ones (sketched in Fig. 9), we simply indicate with $e_x$ the ellipsoid axis along the $x$ direction, and similarly for the others. The lengths $l_x$ and $l_y$ of the ellipsoid semi-axis, on $e_x$ and $e_y$ respectively, are a measure of the ability of the hand to move the object in the relative direction, while $l_z$ is a measure of the ability to rotate the object around

[1]For more details about the quasi-static grasp model equations and the manipulability analysis, the reader can refer to [18].

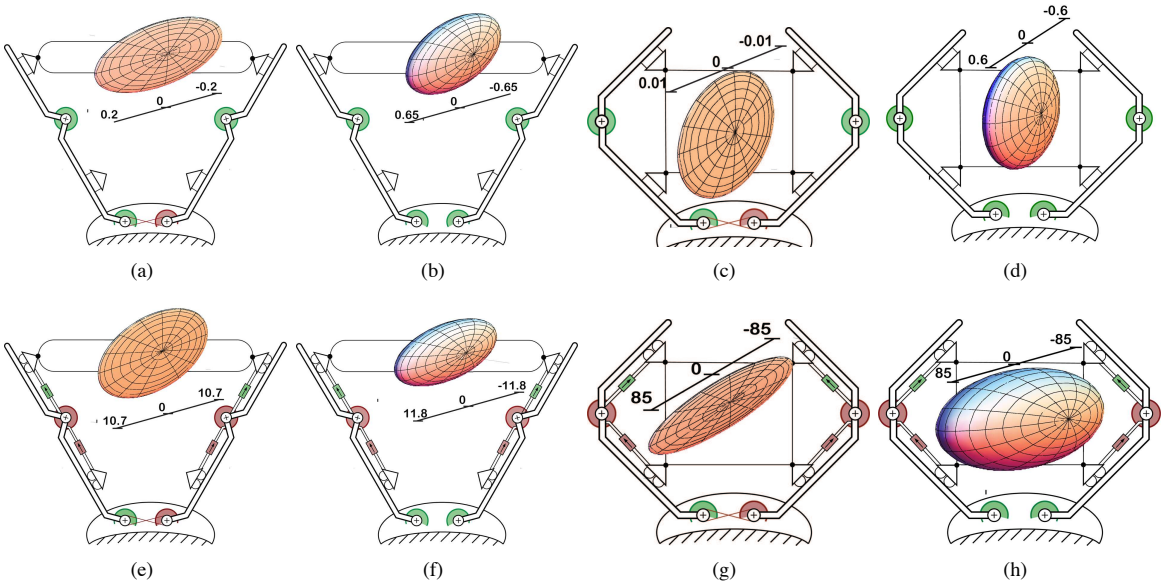


(a) (b) (c) (d) (e) (f) (g) (h)

Fig. 11. Manipulability ellipsoids in different cases. Actuated joints are green, driven joints are red. Manipulation dexterity of four different hands with same structure and same number of DoA are compared. Manipulability ellipsoids of hands with active surfaces (bottom row) is greatly increased whit respect to hands where the same number of DoAs are used elsewhere in the joints (top row). Refer to TABLE I for ellipsoid (ellipsis) characteristic dimensions.

| Figure | Type | $e_x$ | $e_y$ | $e_z$ | Volume (Area) |
|---|---|---|---|---|---|
| 11(a) | TNa3 | none | 0.03 | 0.2 | 0.188 |
| 11(b) | TNa4 | 0.001 | 0.01 | 0.65 | $2.7(10)^{-5}$ |
| 11(c) | PNa3 | none | 0.001 | 0.01 | $3.1(10)^{-5}$ |
| 11(d) | PNa4 | 0.01 | 0.1 | 0.6 | 0.0025 |
| 11(e) | TA3 | none | 0.45 | 10.7 | 15.1 |
| 11(f) | TA4 | 0.01 | 0.5 | 11.8 | 0.24 |
| 11(g) | PA3 | none | 0.25 | 85 | 66.7 |
| 11(h) | PA4 | 0.1 | 0.25 | 85 | 8.9 |

TABLE I

ELLIPSOID AXIS LENGTHS AND VOLUMES (OR AREAS OF THE ELLIPSIS).

$e_z$. As expected numerical results show how, in the cases of 3 DoAs, ellipsoids collapse into ellipsis. In all cases from Table I we can observe that, given the grasp configuration (power grasp or tip grasp) and the number of DoAs we always obtain an axial length increase. The advantage of the solution with active surfaces is highlighted by a two orders of magnitude growth of the ellipsoid volumes (or ellipses areas in the 3 DoA cases), implying a higher dexterity of the hand in manipulating the object.

## IV. VELVET FINGERS IMPLEMENTATION

In the overall view of Fig. 13 three main mechanical subsystems can be discerned: a palm and, for each finger, one proximal and one distal phalanxes[2]. Each one of the two fingers can be seen as a planar RR manipulator. The hand is under-actuated, one motor actuates closure and other two active surfaces of each finger. Cut view of finger (1) shows the mechanical transmission for the hand closure, whereas within finger (2) the transmission system of the conveyor belt, which implements the active surface, is shown. The gripper closure is actuated by motor (4) that, by means of gears (6) and (7), transmits the motion to the two fingers. The movement of the pulley (21), idle w.r.t proximal 1, is conferred by timing belt (B1). Motion transmission from pulley (21) to pulley (32), fixed on the distal 1, is conferred by timing belt (B3). The rotation of proximal 1 is conferred by the tension springs (27) that links it to distal 1. The actuator (4) is a $6W$ Maxon RE-MAX brushed DC motor with nominal torque $6.82\,mNm$ (peak torque $27.8\,mNm$) with a 316:1 gearbox able to exert a maximum continuous force of $12.6N$ on the tip of distal 1 (about $50N$ in peak torque condition). Hence the hand is able to grasp a mass of about $1\,kg$ and lift it with an acceleration of $1\,g$.

Fig. 12(a) shows the configuration of completely open hand. The implemented transmission design ensures, without external interactions, a V-shaped closure of the fingers, with both the second joint variables $q_2$ equal to zero. Moreover,

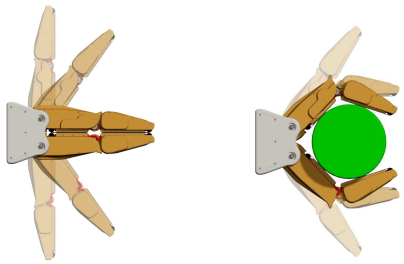

(a) (b)

Fig. 12. Free hand closure movement (left) and constrained enveloping closure around a cylindrical object (right).

[2]In this section the notation (*number*) refer to the identification number of components.

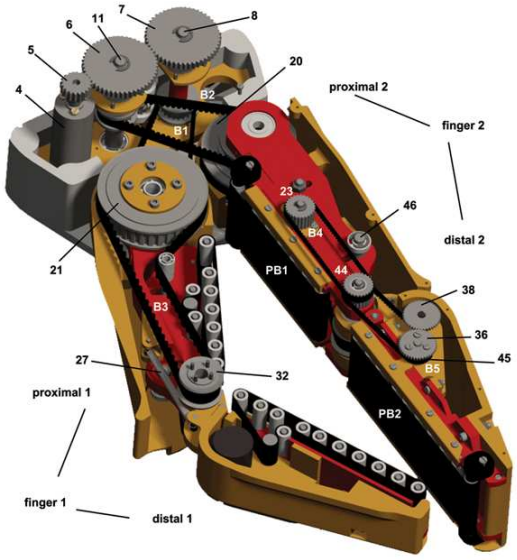


Fig. 13. Cut view of the hand. Section of the palm shows the transmission between the rotational joint actuation unit (11) and (8) and the free pulleys (20) and (21) mounted on the proximal phalanges. The transmission is obtained by a combination of linear spur gears (5), (6), (7) and timing belts (B1 and B2). Section of finger 1 shows the transmission between the free pulley (21) and the pulley (32) fixed on the distal phalanx.

an end-stroke between proximal 1 and distal 1 ensures a minimal value of $q_2$ equal to zero. On the other hand, if contact forces block the first link, the distal tends to rotate w.r.t. proximal determining an enveloping grasp (see Fig. 12 (b)).

Both active surfaces on the two links are $40\,mm$ wide conveyor belts actuated in the same verse by a same motor (38). The transmission to implement this is composed of timing belts (B4) and (B5) and pulleys (23), (44) and (45). The pretension of belts (B4) and (B5) is given by the tightener (46) and the mobile support of the motor (38) respectively.

### A. Palm

Fig. 14 shows a detailed 3D view of the palm. Pinion (5), actuated by motor (4), transmits the motion to the spur gear (6) (transmission ratio -1:2.5), which engages also with gear (7) (transmission ratio -1:1). Gears (6) and (7) rotate, via shafts (11) and (8), timing pulleys (10) and (9) respectively. Each pulley, by means of timing belts (B2) and (B1) (tensioned by tighteners (12) and (13)), transmits the movement to a finger, realizing a 5:1 total transmission ratio between the motor (4) and the finger pulley (20). The angular position of shaft (11) is measured by a magnetic encoder composed of a magnet (14) and a sensor (15) fixed on the extremity of the shaft. Two electronic boards, fixed at the bottom of the palm, drive the motors and read the sensors.

### B. Proximal Phalanx

Fig. 15 shows a 3D section of the proximal phalanx. Pulleys (20) and (21), fixed each other, are idle on axis (19) which is fixed on the palm ((1) on Fig. 14). Pulley (20) receives motion from pulley (10) with transmission ratio 1:2,

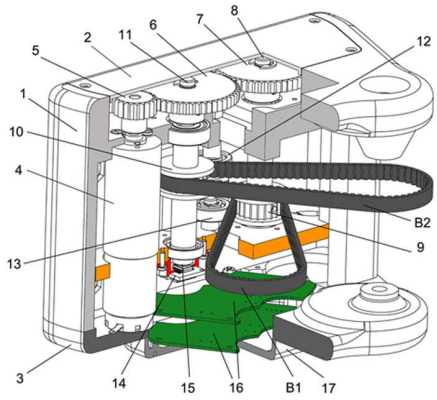


Fig. 14. 3D section of the palm. Transmission belts (B1) and (B2), gears (5), (6), (7), sensors (14) and (15) and electronic boards (16) are highlighted. One DoA can be added to the hand, decoupling the two finger motions, by mounting one more motor inside the palm frame (1), symmetrically to motor (4). In this configuration gear (8) must be inverted, avoiding the engaging with gear (6).

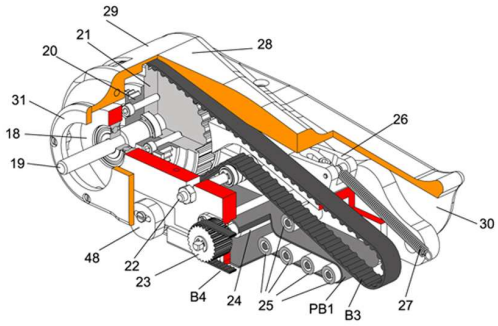


Fig. 15. 3D section of the proximal phalanx. Belts (B3) and (B4) and the conveyor system are highlighted. Pulleys (21) and (20) are free to rotate around the shaft (19), fixed on palm frame (1), they are an interconnection in the transmission chain between the motor (4) and the distal phalanx. Proximal phalanx is mounted on shaft (19) by two ball bearings.

whereas pulley (21) transmits motion to the pulley fixed on the second link through belt (B3), tensioned by tightener

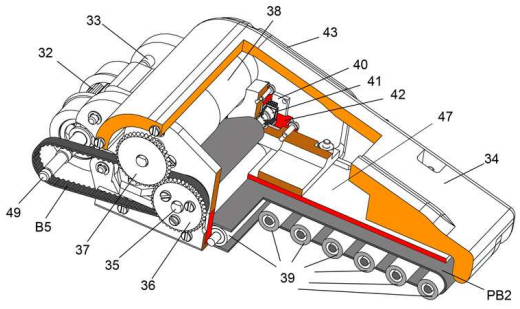


Fig. 16. 3D section of the distal phalanx. Details about conveyor system and its actuation are shown. Belt (B5) transfers motion from the conveyor on the distal phalanx to the conveyor on the proximal phalanx. Motor (38) is mounted on a mobile frame that can be shifted, along some grooves on frame (47), to tighten plain belt (PB2).

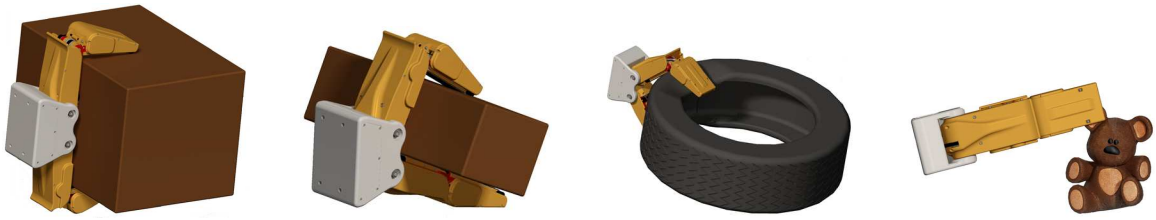

(a) (b) (c) (d)

Fig. 17. Examples of grasps obtained with the "velvet fingers" dexterous gripper. Grasped objects are part of the scenario of the EU founded project ROBLOG (`www.roblog.eu`), for which this EE has been designed. The objects grasped are: a big box 390x290x270mm (a), a small box 376x149x122 mm (b), a tire P195/55R16 85H (c) and Teddy bear (d).

(22). The distance between the joint axes is 128mm.

At the bottom of the first link plain belt (PB1) wraps around 8mm diameter rollers (25), mounted by ball bearings on steel pins. Pulley (23) moves the motor roller (24) that actuate the plain belt. A mobile roller (48) provides the right pretension to (PB1).

### C. Distal Phalanx

Frame (34) of the distal phalanx (about 132 mm long) in Fig. 16 is mounted through ball bearings on the pin (49) (fixed on frame (18) of the proximal phalanx), and it is rigidly connected to pulley (32). Springs (27) are hooked on frame (34) by the pin (33). Conveyor belt (PB2) wraps around rollers (39) and is pretensioned by a mobile roller (similar to (48) in Fig. 15), on the tip of the phalanx. The movement of the plain belt is conferred by motor (38) to the motor shaft (35) through a transmission gear. At the end of shaft (35) a magnetic encoder (40) is fixed for belt position sensing. Actuator (38) is the same of (4), with a 4.4:1 reduction, so it can exert a force on the belts of about 30N.

## V. CONCLUSIONS

The hand proposed in this paper combines the robustness and control simplicity of an under-actuated gripper with the dexterity of an high DoA robotic hand, able to assure a stable grasp combined with an high manipulation capacity. This improvement is obtained thanks to the application of active surfaces to the gripper finger-pads. A manipulability analysis is provided to highlight the introduced dexterity advantage, pointing out a significant increase of the manipulability ellipsoid's dimension. A mechanical description of the device, which prototype is currently under development, has been presented. Finally, Fig. 17 shows some static grasping possibilities of the gripper, while Fig.s 3, 4, 5, 6 show the gripper enhanced dexterity.

## VI. ACKNOWLEDEGEMENT

The authors gratefully acknowledge the contribution of Marco Gabiccini, Fabio Bonomo, Andrea di Basco and Fabrizio Vivaldi for their support and useful work. The research leading to these results has received funding from the European Union Seventh Framework Programme [FP7/2007-2013] under grant agreements n ICT-270350 (project ROBLOG) and ERC Advanced Grant 291166 (SoftHands).

## REFERENCES

[1] G. Monkman, S. Hesse, and R. Steinmann, *Robot grippers*. Vch Verlagsgesellschaft Mbh, 2007.

[2] M. T. Mason and J. K. Salisbury, *Robot Hands and the Mechanics of Manipulation*. MIT Press Cambridge, MA, 1985.

[3] S. Jacobsen, E. Iversen, D. Knutti, R. Johnson, and K. Biggers, "Design of the utah/mit dextrous hand," in *Robotics and Automation. Proceedings. 1986 IEEE International Conference on*, vol. 3. IEEE, 1986, pp. 1520–1532.

[4] A. Dollar and R. Howe, "Simple, robust autonomous grasping in unstructured environments," in *Robotics and Automation, 2007 IEEE International Conference on*. IEEE, 2007, pp. 4693–4700.

[5] F. Ficuciello, G. Palli, C. Melchiorri, and B. Siciliano, "Experimental evaluation of postural synergies during reach to grasp with the ub hand iv," in *Intelligent Robots and Systems, IROS*, 2011.

[6] M. Grebenstein, A. Albu-Schaffer, T. Bahls, M. Chalon, O. Eiberger, W. Friedl, R. Gruber, S. Haddadin, U. Hagn, R. Haslinger, H. Hoppner, S. Jorg, M. Nickl, A. Nothhelfer, F. Petit, J. Reill, N. Seitz, T. Wimbock, S. Wolf, T. Wusthoff, and G. Hirzinger, "The dlr hand arm system," in *Robotics and Automation (ICRA), 2011 IEEE International Conference on*, may 2011, pp. 3175 –3182.

[7] A. M. Okamura, N. Smaby, and M. Cutkosky, "An overview of dextrous manipulation," in *IEEE International Conference on Robotics and Automation San Francisco, CA*, 2000, pp. 255–262.

[8] K. B. Shimoga, "Robot grasp synthesis algorithms: A survey," *International Journal of Robotics Research*, pp. 230–266, 1996.

[9] A. M. Dollar and R. D. Howe, "The highly adaptive sdm hand: design and performance evaluation," *The international journal of robotics research*, 2010.

[10] L. Birglen, C. Gosselin, and T. Laliberte, *Underactuated robotic hands*. Springer Verlag, 2008.

[11] C. Brown and H. Asada, "Inter-finger coordination and postural synergies in robot hands via mechanical implementation of principal components analysis," in *Intelligent Robots and Systems, IROS*, 2007, pp. 2877–2882.

[12] A. Bicchi, M. Gabiccini, and M. Santello, "Modelling natural and artificial hands with synergies," *Philosophical Transactions of the Royal Society B: Biological Sciences*, 2011.

[13] K. Autumn, A. Dittmore, D. Santos, M. Spenko, and M. Cutkosky, "Frictional adhesion: a new angle on gecko attachment," *Journal of Experimental Biology*, vol. 209, no. 18, p. 3569, 2006.

[14] S. Kim, M. Spenko, S. Trujillo, B. Heyneman, D. Santos, and M. Cutkosky, "Smooth vertical surface climbing with directional adhesion," *Robotics, IEEE Transactions on*, vol. 24, no. 1, pp. 65–74, 2008.

[15] J. Lindsay, F. Chen, L. Yu, and N. Efremova, "Nanofabricated gecko-like fasteners with adhesive hairs for disposable absorbent articles," Oct. 12 2010, uS Patent 7,811,272.

[16] J. Dejeu, M. Bechelany, P. Rougeot, L. Philippe, and M. Gauthier, "Adhesion control for micro-and nano-manipulation," *ACS nano*, 2011.

[17] A. Bicchi, C. Melchiorri, and D. Balluchi, "On the mobility and manipulability of general multiple limb robots," *IEEE Transaction on robotics and automation*, 1995.

[18] D. Pratichizzo, M. Malvezzi, and A. Bicchi, "On motion and force controllability of grasping hands with postural synergies," in *Robotics: Science and Systems*. IEEE, 2010.

[19] A. Bicchi and R. Sorrentino, "Dexterous manipulation through rolling," in *Int. Conf. on Robotics and Automation*. IEEE, 1995, pp. 452–457.